Finite element modeling of sound transmission from outer to inner ear

Bruno Areias; Carla Santos; Renato Natal; Fernanda Gentil; Marco Parente

Abstract

The human ear is a complex organ in our organism. Sound is a sequence of waves of pressure, which propagates through compressible media such as air. The pinna concentrates the sound waves into the external auditory meatus. In this canal the sound is conducted to the tympanic membrane. The tympanic membrane transforms the pressure variations into mechanical displacements, which are then transmitted to the ossicles. The vibration of the stapes footplate creates pressure waves in the fluid inside the cochlea, this pressure waves stimulate the hair cells and then these stimulations are send to the brain via cochlear nerve, where will be decoded [1].

The external auditory meatus set up a communication between the external environment and the middle ear. This canal has approximately 25 mm in length and 8 mm in diameter [2], has tapered shape along their length and a curved path which varies between individuals. The relation between the dimensions of the canal, and the wavelength of sound should be taken into account in the phenomenon of acoustic transmission from the entrance of canal to the tympanic membrane. Below 1 kHz, the wavelengths are much larger than any external auditory meatus dimensions, so small variations in the canal dimensions are unimportant. However, at 10 kHz the wavelength is 34 mm, which is approximately four times the diameter of the tympanic membrane. On these frequencies are expected which variations of cross section or canal curvature become significant in the sound transmission [3].

In this work is developed a 3D finite element of the human ear, the model incorporates the tympanic membrane, ossicular bones, part of temporal bone (external auditory meatus and tympanic cavity), middle ear ligaments and tendons, cochlear fluid, skin, ear cartilage, jaw, and the air in external auditory meatus and tympanic cavity.

Through the element finite method is calculated the magnitude and the phase angle of the umbo and staples displacement for the model with and without the air in the external auditory meatus. The middle ear sound transfer function is determined for a stimulus of 60 dB SPL, applied on the outer surface of the air in external auditory meatus. The model results were also compared with previously published data in the literature. A study about the importance of external auditory meatus is performed. The pressure gain is calculated for the external auditory meatus. The frequency band in study is between 100 Hz and 10 kHz.

Keywords

Finite element model; Tympanic cavity; Biomechanics; Acoustics; Hearing

Introduction

Hearing is one of the five senses in humans, and one of the most important for your social life or even for your survival. Hearing loss can induce a severely disabling disease. The human ear is a complex organ which allow understand and interpret the sound waves at frequency band between 16 Hz and 20 kHz, and intensities between 0 dB and 130 dB. It's responsible for our equilibrium, having a particular sensitivity to transform the sound waves into electrical signals, and transmit them after to the brain, through the auditory nerve. The ear is almost totally located in the temporal bone, positioned at the base and sidewall of the skull [4].

Some authors describe the normal ear behaviour [5-9], whereas others reproduced the different pathologies associated with the middle ear [10-15].

Gan *et al.* [6] elaborate a full finite element model. The cochlea is composed of vestibular and tympanic scale, and separated by basilar membrane. The middle ear transfer function, the umbo and stapes displacement and cochlear impedance are obtained in this study.

Yingxi Liu *et al.* [10] develop a finite element model that incorporate the tympanic membrane, ossicular bones, middle ear ligaments and tendons, external auditory meatus, tympanic cavity and the cochlear fluid. The numerical study of Yingxi Liu *et al.* [10] predict the effects when different types of diseases affect the human ear, such as, malleus handle defect, hypoplasia of the long process of incus, and stapedial crus defect.

Gentil *et al*. [14] investigate the effect of tympanic membrane perforations and myringosclerosis in the mechanical behaviour of the tympano-ossicular chain. Using the finite element method concluded, that when the microperforation (0.6 mm) is present, no differences in terms of the umbo or stapes footplate displacement are seen, compared with the normal tympanic membrane. The largest differences occur with a perforation of 7.0 mm, the results showing a decrease of the displacements at low and medium frequencies.

The aim of this work is study the functioning of the human ear using numerical analysis. Will be simulated numerically the transmission of sound from the pinna to the stapes. The geometric models developed in this study, were based on the project “The visible ear”. The main objective of this project was to develop a high resolution digital atlas of the temporal bone. The images used to create the atlas, were obtained using the procedure cryosectioning to the temporal bone of a woman with 85 years old. Finally, hand-segmentation of the different tissues was performed [16].

In this study, the full model consists in the simple model added by the air in the external auditory meatus and tympanic cavity. Comparisons between both models allows explain numerically the influence of the external auditory meatus on human auditory system. Model validation is confirmed by comparison of the umbo and stapes displacement in the simple model, with experimental and numerical results previously published in literature. An acoustic-mechanical analysis is presented by introducing the air in the external auditory meatus and in the tympanic cavity. The middle ear sound transfer function and the pressure gain of the external auditory meatus was determined to the full model.

Materials and Methods

Construction of FEM 3D

The geometric models developed had origin in the project “The Visible Ear”. A set of high quality images, of the frozen temporal bone are obtained through cryosectioning tissues procedure. The slice thickness was 25 µm and high resolution images were captured every 50 µm. A total of 597 imagens with 24 bits RGB and a resolution of 50 µm/pixel were obtained. About 26 different organs of middle ear were identified through manual segmentation performed by Mads Sølvsten Sørensen of each image [16]. Based on this project the geometric model of the tympanic membrane, ossicular bones, cochlea, external auditory meatus, tympanic cavity, and other parts that formed the model in this work was extracted.

In the developed model the influence of external auditory meatus was studied, were performed two geometric models (see Figure 1). The simple model compound by the tympanic membrane,

ossicular bones (malleus, M; incus, I; stapes, S1), cochlea (CF), two tendons (stapedius tendon (ST) and tensor tympani tendon (TT)), six ligaments (superior mallear ligament, SML; lateral mallear ligament, LML; anterior mallear ligament, AML; superior incudal ligament, SIL; posterior incudal ligament, PIL; stapedius annular ligament, SA), incudomalleolar (IMJ) and incudostapedial joint (ISJ), and part of temporal bone (TB). The full model is formed by the simple model added by the air in external auditory meatus (EAM) and tympanic cavity (TC), skin (S2), jaw and ear cartilage (EC).

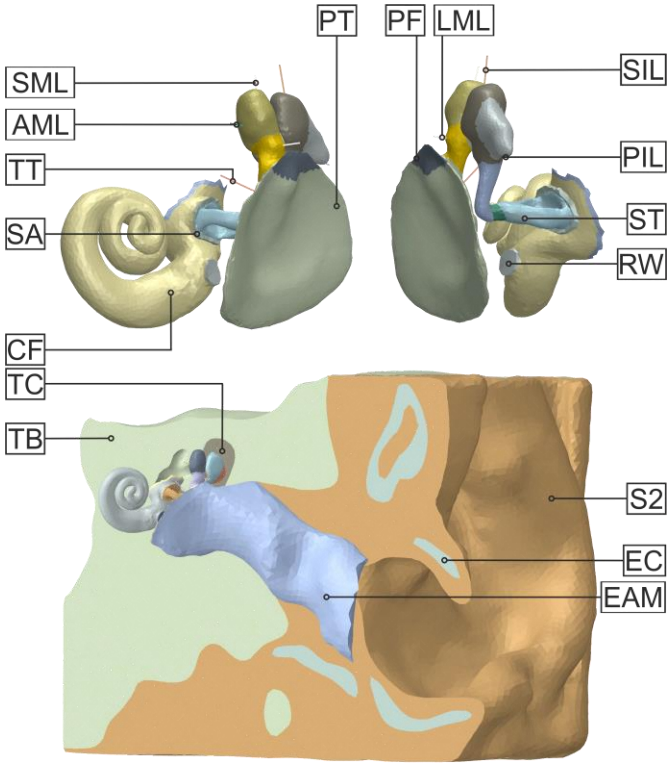

Figure 1. Simple model without temporal bone (top) and full model sectioned (down).

The finite element mesh and the numerical simulations were carried out using the software commercial *Abaqus® Standard* [17].

The model was discretized with 255 343 nodes and 1 345 379 elements, of which 1 186 243 linear tetrahedral (C3D4) elements, 159 129 linear tetrahedral acoustic (AC3D4) elements and 7 linear truss (T3D2) elements. The tendons and ligaments were simulated through truss elements of type T3D2, the acoustic components are meshed with acoustic elements of type AC3D4 and the remaining parts of the ear with tetrahedral elements of type C3D4.

The Eustachian tube was considered closed on the connection with the nasopharynx.

Material properties

The middle ear has been described as a linear system for transmission acoustic-mechanical from the tympanic membrane to the cochlea [5, 7, 13, 18]. Mechanical properties were incorporated in all parts of the 3D finite element model. The Poisson's ratio is assumed to be 0.3 for all parts of the human ear [13, 18], except in the ear cartilage which was assumed 0.4 [19].

Raleigh's proportional damping was introduced in the middle ear components, with the coefficients $\alpha = 0\ \mathrm{s}^{-1}$ e $\beta = 0.0001\ \mathrm{s}$. The Raleigh damping matrix, C, is expressed as a combination of stiffness and mass matrix, and is obtained as follows:

$$C = \alpha M + \beta K,$$

where M is the mass matrix, K, the stiffness matrix, and α and β, the Raleigh damping coefficients.

Tympanic membrane was assumed homogeneous with orthotropic behaviour in *Pars tensa* and isotropic behaviour in *Pars flaccida* [5, 8, 13-15, 20, 21]. The radial and circumferential Young's modulus was 32 MPa and 20 MPa in *Pars tensa*, respectively. The Young's modulus was 10 MPa in *Pars flaccida*.

The ossicular bones were assumed with homogeneous and isotropic behaviour. The Young's modulus for the three ossicles were 14,1 GPa and the density are shown in Table 1.

The joints, skin, ear cartilage, temporal bone, jaw and the round window were assumed homogeneous and isotropic with properties listed in Table 1.

Table 1. Material properties of ear components

Ear components	$\rho\ \left[\frac{kg}{m^3}\right]$	E [Pa]	Damping
Tympanic membrane (TM) [13]	1.2×10^3	Pars tensa (**PT**) 3.2×10^7 (radial) 2.0×10^7 (circunferential) Pars flaccida (**PF**) 1.0×10^7 (radial) 1.0×10^7 (circunferential)	$\alpha = 0\ s^{-1}$ $\beta = 0.0001\ s$
Malleus (M) [13]	2.55×10^3 (Head) 4.53×10^3 (Neck) 3.70×10^3 (Handle)	1.41×10^{10}	
Incus (I) [13]	2.36×10^3 (Body) 2.26×10^3 (Short process) 5.08×10^3 (Long process)	1.41×10^{10}	
Stapes (S1) [13]	2.2×10^3	1.41×10^{10}	
Incudomalleolar Joint (IMJ) [13]	3.2×10^3	1.41×10^{10}	
Incudostapedial Joint (ISJ) [13]	1.2×10^3	6.0×10^5	
Skin (S2) [19]	1.2×10^3	$1{,}67 \times 10^7$	
Ear cartilage (EC) [19]	1.2×10^3	$2{,}5 \times 10^7$	
Temporal bone (TB) and Jaw	2.0×10^3	1.41×10^{10}	
Round window (RW)	1.2×10^3	1.0×10^7	

The ligaments that suspend the ossicles, and the tendons that protect the ear from loud sounds, were assumed to be linear elastic as shown in Table 2. The density and Rayleigh damping coefficients are displayed in Table 2. Figure 2 shows the boundary conditions applied to the tympanic membrane and the staples. The tympanic annulus (TA) is inserted into the temporal bone [20], and was assumed an isotropic behaviour with Young's modulus of 6.0×10^4 Pa. The stapedius annular ligament was also assumed with isotropic behaviour as shown in Table 2.

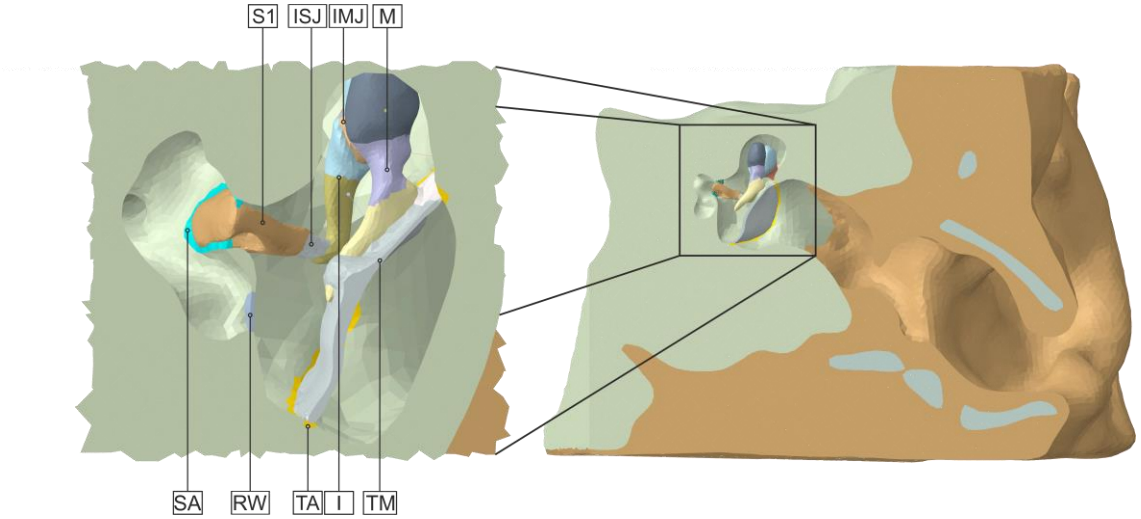

Figure 2. Representation of stapedius annular ligament and tympanic annulus.

Table 2. Material properties of ligaments and tendons

Ligaments and tendons	$\rho\ \left[\frac{kg}{m^{-3}}\right]$	E [Pa]	Damping
Superior mallear ligament (SML) [9, 13]	2.5×10^3	4.9×10^4	$\alpha = 0\ s^{-1}$
Lateral mallear ligament (LML) [9, 13]	2.5×10^3	6.7×10^4	$\beta = 0.0001\ s$
Anterior mallear ligament (AML) [9, 13]	2.5×10^3	2.1×10^6	
Superior incudal ligament (SIL) [9]	2.5×10^3	4.9×10^4	
Posterior incudal ligament (PIL) [9, 13]	2.5×10^3	6.5×10^5	
Tensor tympani tendon (TT) [9, 13]	2.5×10^3	2.6×10^6	
Stapedius tendon (ST) [9, 13]	2.5×10^3	5.2×10^5	
Tympanic annulus (TA)	1.2×10^3	6.0×10^4	
Stapedius annular ligament (SA)	2.5×10^3	2.0×10^4	

The air in external auditory meatus and in tympanic cavity, and the fluid inside the cochlea were modelled as acoustic elements. The constitutive behaviour of the fluid is described by the equation:

$$p = -K_f \varepsilon_v$$

which presupposes that the fluid is inviscid, linear and compressible. In this equation p, is acoustic pressure, ε_v is the volumetric strain, K_f, the bulk modulus defined by the formula $K_f = c^2\rho$, where c is the speed of sound in a medium, and ρ, the density of fluid.

The properties for the acoustic medium are displayed in Table 3.

Table 3. Acoustic properties of ear components

Acoustic medium	$\rho\ \left[\frac{kg}{m^{-3}}\right]$	B [Pa]
Air (EAM;TC)	1.164	1.01×10^5
Cochlear fluid (CF) [6]	1000	220×10^9

In the simple model the acoustic pressure is applied at tympanic membrane, whereas the full model the same pressure is applied on the outer surface of the air in external auditory meatus, as shown in Figure 3.

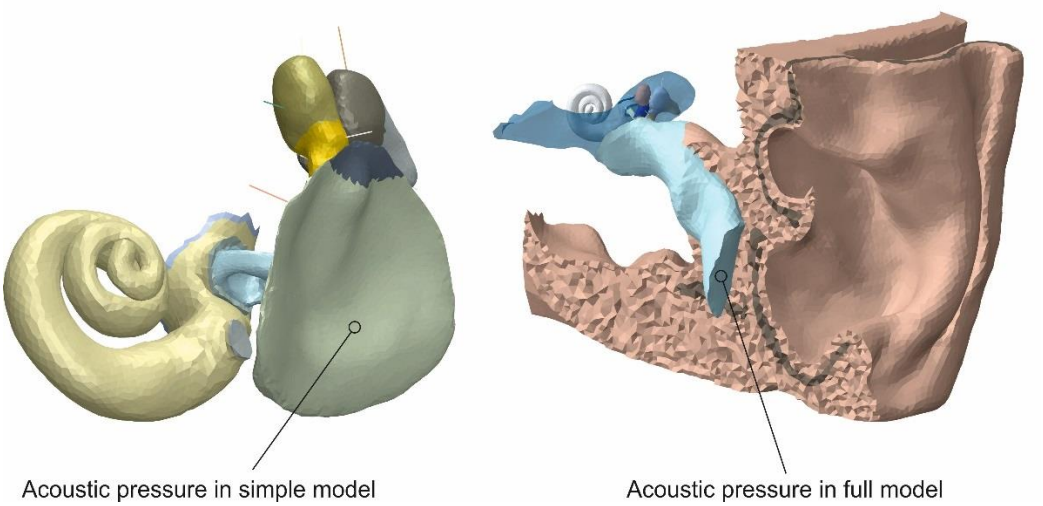

Figure 3. Places of application the pressure in both developed models.

Boundary conditions

In both models, the part of the temporal bone and jaw sectioned is fixed in all freedom, thus considering an encastre boundary condition (the red points in Figure 4 shows the location of this boundary condition). The connection between the acoustic elements and the structural elements of the ear was performed using the *TIE* command available in *Abaqus® Standard* [17]. This option allows impose acoustic-mechanical interactions between pairs of surfaces.

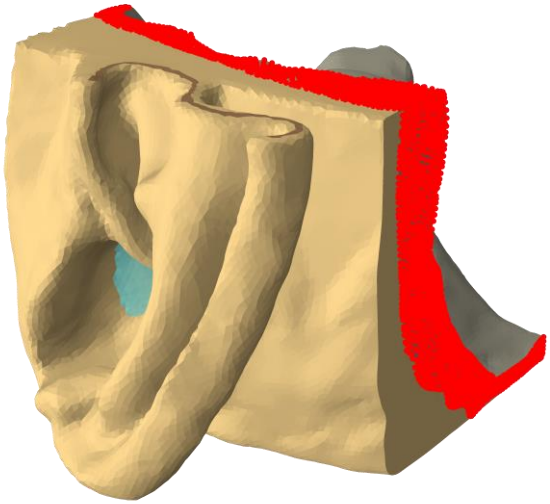

Figure 4. Boundary conditions.

Results

Figure 5 and Figure 6 show the frequency response of displacement at the umbo and stapes footplate in the simple model, respectively. In this analysis a sound pressure level of 80 dB SPL at tympanic membrane is applied (black solid line). Figure 5a and Figure 6a show the magnitude of displacement whereas Figure 5b and Figure 6b the phase angles. Model validation was performed by comparison of the responses obtained with experimental results published by Nishihara *et al*. [22] and Huber *et al*. [23], and also, through comparison with numerical results obtained by Chia *et al*. [24] and Gentil *et al.* [9]. In the study of Nishihara *et al.* [22], the experimental data were obtained from 64 individuals with normal hearing. Thirty-four different

tones at 80 dB SPL in the frequency band 195 Hz to 19433 Hz at tympanic membrane were induced, and the displacement at the umbo using a laser instrument were measured. Huber *et al.* [23] published a study with experimental displacement data at the umbo and stapes footplate obtained from 10 temporal bones. Chia *et al*. [24] simulate through finite element method the middle ear, formed by tympanic membrane and ossicular bones. In the work of Gentil *et al.* [9] the displacement at the umbo and stapes footplate for a sound pressure level of 80 dB SPL are determined, Gentil *et al.* [9] employ a model formed by the tympanic membrane, ossicular bones, and consider the ligaments and muscles with hyperelastic behaviour. Gan *et al.* [6] develop a FE model of human ear where the sound pressure is applied to 2 mm from tympanic membrane. The phase response at umbo and stapes footplate is obtained and is shown in Figure 5b e Figure 6b, respectively. The values achieved for the phase of the stapes footplate are in agreement with those obtained by Gan *et al*. [6], which tends to decrease up to 300° with increasing frequency. Based on obtained data, the Figure 6a shows that the magnitude of stapes footplate displacement increase up to 700 Hz, from this value there are a decrease of the displacement until the end of the frequency band studied.

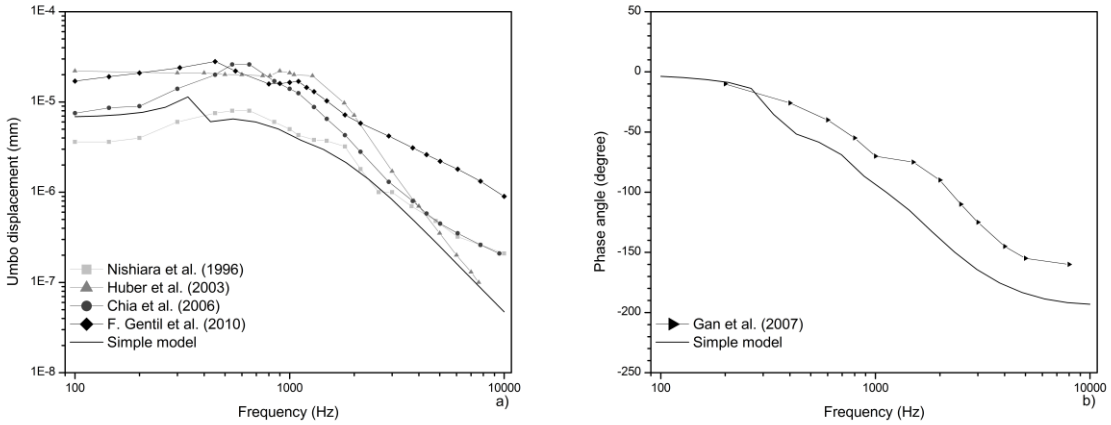

Figure 5. Umbo displacement for 80 dB SPL applied to the tympanic membrane; (a) Magnitude; (b) Phase angle.

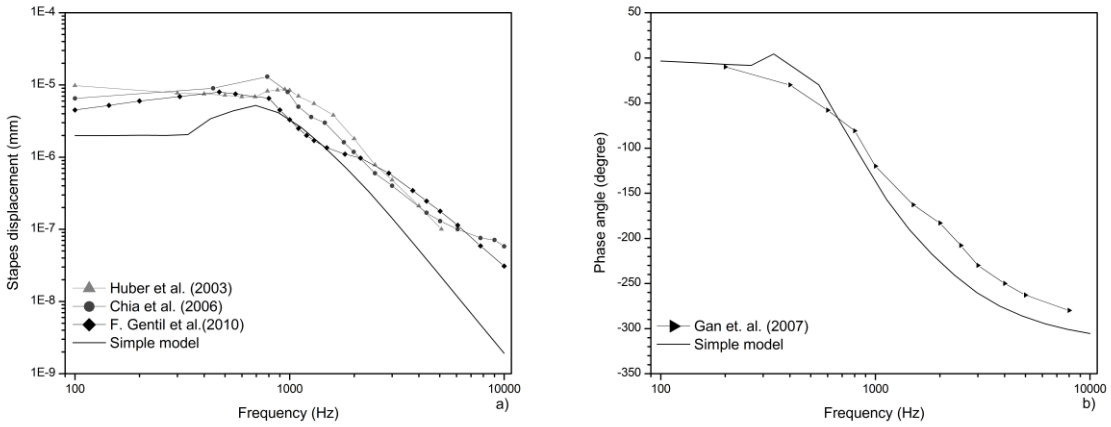

Figure 6. Stapes footplate displacement for 80 dB SPL applied to the tympanic membrane; (a) Magnitude; (b) Phase angle.

The full model is formed by the simple model added by the air in external auditory meatus and in the tympanic cavity. A study involves the comparison of the umbo and stapes footplate displacement between both models. Figure 7 and Figure 8 show the results obtained (magnitude (a) and phase angles (b)) for the displacements at the umbo and stapes footplate. In the simple

model the acoustic pressure is applied to the tympanic membrane whereas in the full model the same pressure is applied on the outer surface of the air in external auditory meatus entrance (see Figure 3). The results obtained for the full model (black broken line) highlights the important role that external auditory meatus has in amplify the sound at the high frequencies. In the umbo and stapes footplate displacement was checked a phase shift of 180° near 3 kHz, which shows an acoustic resonance near that frequency in external auditory meatus. The first resonance frequency of external auditory meatus varies with the individual age, decreasing with an increase in age. In the Figure 7 and Figure 8 is also represented the numerical results published by Prendergast *et al*. [12], which presupposes a resonance peak at 4 kHz associated with the external auditory meatus. Bentler [25] published experimental data of acoustic pressure distribution along the external auditory meatus based on 78 children with ages between 3 to 13 years. The average resonance frequency of external auditory meatus was 2848 Hz with a gain of 18.9 dB. The experimental data of Shaw [26] were measured from adult individuals. The first resonance frequency of external auditory meatus occurs near 2600 Hz.

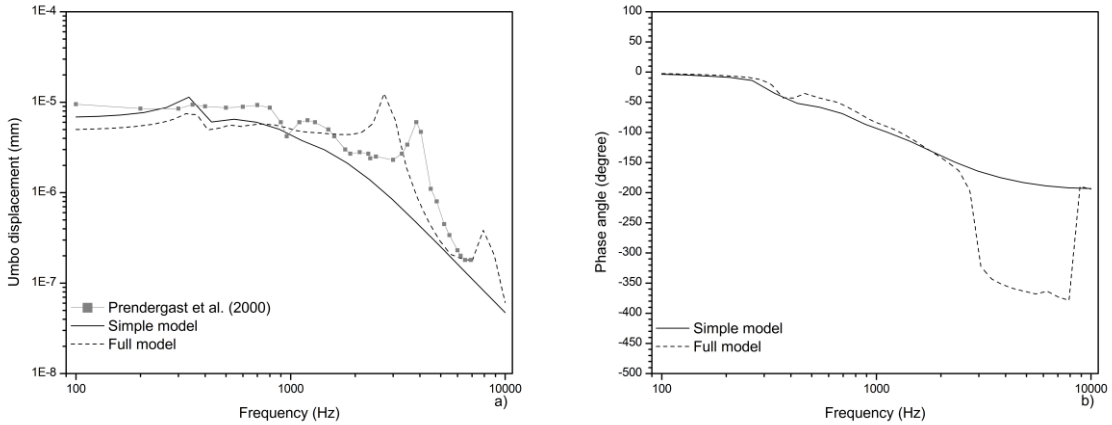

Figure 7. Comparison of displacement at the umbo between simple and full model. The input sound pressure level was 80 dB SPL.

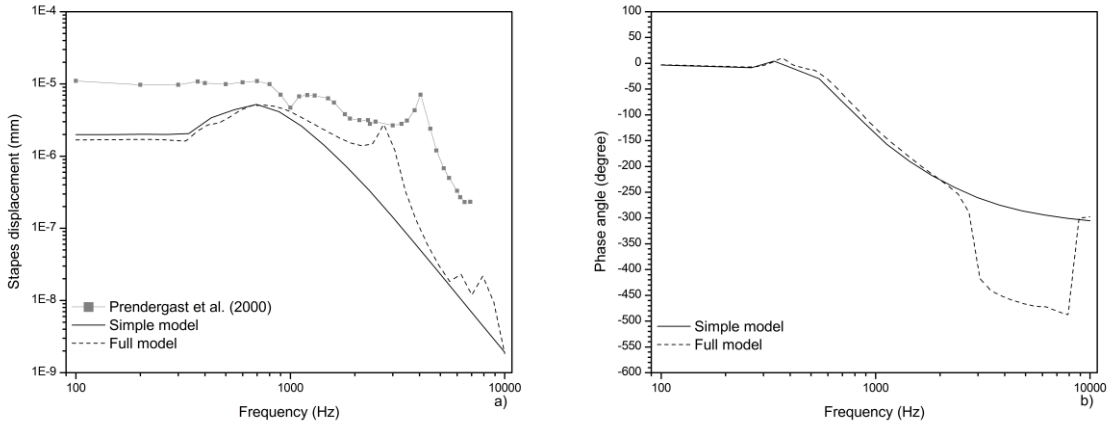

Figure 8. Comparison of displacement at the stapes footplate between simple and full model. The input sound pressure level was 80 dB SPL.

The dynamic behaviour of the middle ear can be characterized using a transfer function calculated through the ratio of stapes footplate velocity and the sound pressure in external auditory meatus close to the tympanic membrane. Figure 9 shows the comparison between the results obtained by the full model for a sound pressure level of 90 dB SPL, and the results

published by other authors. The experimental data reported by Voss *et al*. [27] were obtained from 18 ears without evidence of ear disease. The experimental results of Alibara *et al*. [28] were acquired from 11 temporal bones. The Figure 9 shows the range of values archived. Sun *et al*. [13] and Gan *et al*. [6] resort to finite elements software for describe the behaviour of the human ear. The air in external auditory meatus and tympanic cavity is considered in the model of Gan *et al*. [6]. The calculated transfer function is close to the lower limit reported by Alibara *et al*. [28], however the built model has a more pronounced decrease in high frequencies. Comparing with the published data of Voss *et al*. [27] in the frequency band of 200 Hz to 4 kHz, the values obtained are also in concordance.

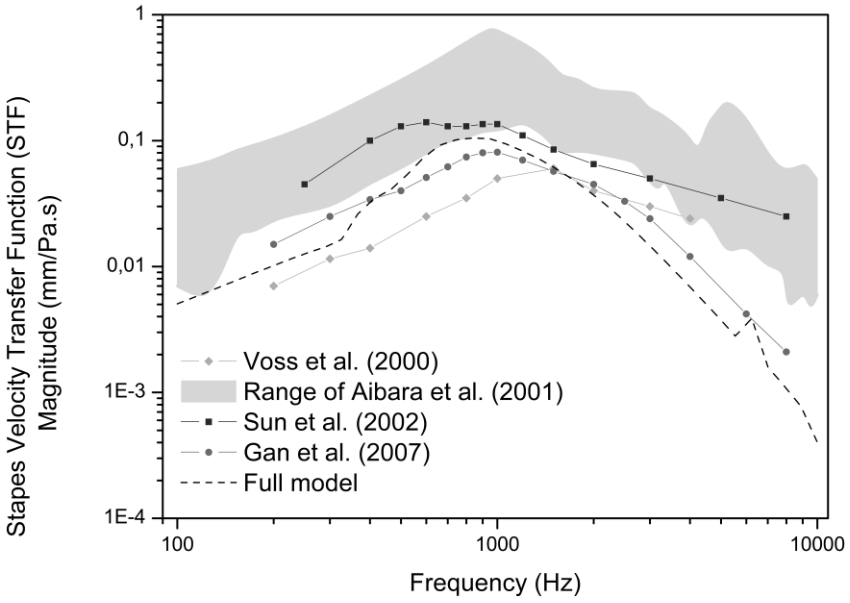

Figure 9. Comparison of the stapes footplate velocity transfer function (STF) with experimental data. The input sound pressure level was 90 dB SPL.

Pressure distribution analysis along the external auditory meatus becomes interesting because this canal contributes significantly for enhancing sound intensity at higher frequencies [7]. The 3D geometry developed of the external auditory meatus has approximately 26 mm in length and an entrance diameter which varies between 6.5 mm and 12.9 mm, corresponding to a canal volume of 1188.5 mm^3. The gain represented in Figure 10, is calculated for the end of external auditory meatus near the tympanic membrane, when a sound pressure level of 60 dB is applied on the outer surface of the air in external auditory meatus. In the developed model was verified the presence of two resonances due to the introduction of the air into the model. The first resonance appears near 3 kHz and the second at 8 kHz (see Figure 10). The maximum gain of 21 dB at 3 kHz is reached. The experimental results published by Wiener *et al.* [29] show the mean ratio of the sound pressure at the eardrum to the free-field pressure averaged, for a number of male observers and measured for various azimuths. The resonance effect of the external auditory meatus results in a peak of about 10 dB near 4 kHz (Figure 10). In the range covered by the tests, this pressure ratio is largely independent of azimuth, as is to be expected. Figure 10 shows also the mean of the experimental result obtained by Mehrgardt *et al.* [30]. In this work the sound distribution in the external auditory meatus was determined for three subjects, the transfer functions from eight points in the ear canal to the eardrum was measured. The impulse

response technique was used for determine the transfer functions, a 33-µsec impulse is fed to a loudspeaker at a distance of about 2.5 m of the subject's head in an anechoic chamber. With the probe tip the impulse response is picked up by a condenser probe microphone. The first resonance of the external auditory meatus is located about 5 kHz and doesn't vary between the subjects, whereas the second resonance varies between 8 and 11 kHz. This anharmonic second resonance is explainable by the inhomogeneity of the ear canal [30, 31]. It's perceptible a perfect similarity at the second resonance frequency with the present numerical study. Hammershoi *et al*. [2] published experimental results obtained from 12 subjects. Concluded that any point between the tympanic membrane and the entrance of the external auditory meatus can be considered independent of direction of the sound incidence.

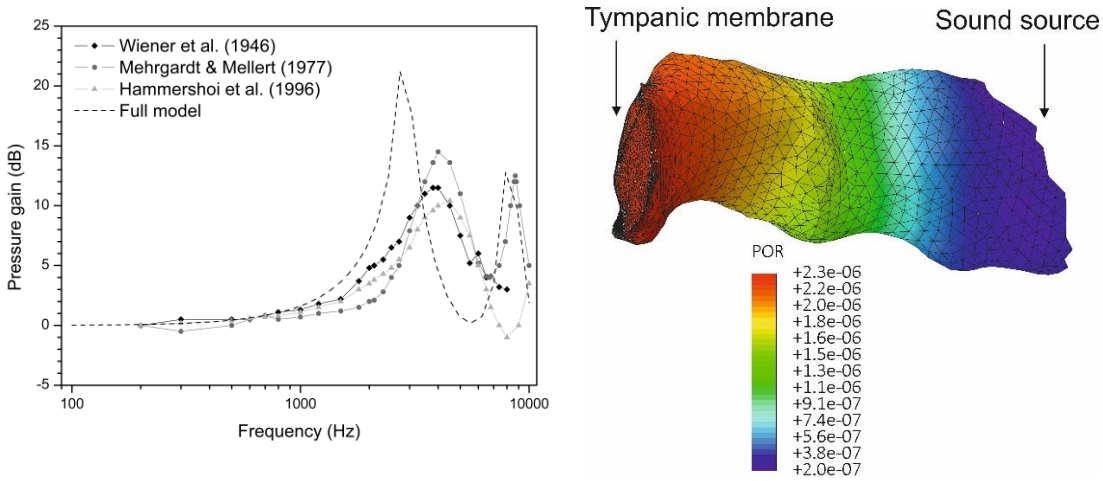

Figure 10. Sound gain in external auditory meatus to 60 dB SPL (left), acoustic pressure distribution [MPa] in external auditory meatus at 2728 Hz and a sound pressure level applied of 60 dB SPL (right).

Conclusions and Discussion

The 3D simple model was validated by comparison of the umbo and the stapes displacement achieved, with other data in literature. The sound pressure level of 80 dB SPL was applied on the lateral surface of the tympanic membrane. The results obtained are close to those published previously in the literature [9, 22-24]. There was an increase in the magnitude of the stapes footplate displacement up to 700 Hz. From this value the displacement began to decrease until the end of the frequency band studied. The phase angle of the stapes footplate is zero at low frequencies, and tends to decrease up to 300°, at 10 kHz.

When introducing the air into the external auditory meatus and into the tympanic cavity, there was a significant gain in sound pressure near of the tympanic membrane. The phase shift of 180° near 3 kHz and 8 kHz, accompanied by a rapid increase of the displacement, show the presence of resonances in external auditory meatus.

The middle ear transfer function calculated from the ratio of the stapes footplate velocity to the sound pressure in external auditory meatus near the tympanic membrane, was compared with published results obtained by other authors. The stapes transfer function curve is close to the lower limit reported by Aibara *et al.* [28], obtained from experimental data.

The temporal bone was considered to be isotropic and wasn't introduced the mastoid process, which inside has air cells [32]. This simplification was due to the low resolution of the 3D atlas in this region, created by hand-segmentation.

The created model of tympanic membrane has a thickness varying between 0.2 mm and 0.5 mm. In literature is verified that most authors adopt an average thickness of 0.074 mm [21]. However, studies such as Kelly *et al*. [33] introduce a membrane with a thickness varying between 0.1 mm and 0.8 mm. The geometric model developed was based on a project, where the procedure for obtaining anatomical geometry is fairly accurate, thus, was considered valid the dimensions reached.

The sound propagates through solid medium, such as the temporal bone, for this reason was introduced this component in the geometric model. The sound waves that cross the skin, ear cartilage, and temporal bone and fall over the inner ear, generating pressure waves in the liquid present inside the cochlea. The pressure waves stimulate the hair cells and then, these stimuli are sent via auditory nerve to the brain, where are decrypted [34, 35]. The model created is composed by the components responsible for the bone conduction, a future study could focus on the influence of this conduction type in the human ear.

A model with the external auditory meatus allows investigate the effects that arise when different pathologies affect the ear canal, such as, obstruction (for example: cerumen), external otitis and tumours. The obstruction of the external auditory meatus can interfere with the passage of sound vibration and affect hearing and communication capabilities of the individual [36, 37].

Acknowledgements

Funding for this work was provided by FCT Grants IF/00159/2014, and research project UID/EMS/50022/2013.

References

1. Bistafa, S.R., *Acústica Aplicada ao Controle do Ruído*. 2011: Editora Edgard Blucher Ltda.
2. Hammershoi, D. and H. Moller, *Sound transmission to and within the human ear canal.* The Journal of the Acoustical Society of America, 1996. **100**(1): p. 408-427.
3. Stinson, M.R., *The spatial distribution of sound pressure within scaled replicas of the human ear canal.* The Journal of the Acoustical Society of America, 1985. **78**(5): p. 1596-1602.
4. Domingues, J., et al., *Anatomia cirúrgica do osso temporal*. 2011: Círculo Médico; Bial.
5. Areias, B.A.F., *Simulação biomecânica do ouvido humano, incluindo patologias do ouvido médio*, in *Engenharia Mecânica*. 2014, Faculdade de Engenharia da Universidade do Porto.
6. Gan, R., B. Reeves, and X. Wang, *Modeling of Sound Transmission from Ear Canal to Cochlea.* Annals of Biomedical Engineering, 2007. **35**(12): p. 2180-2195.
7. Gan, R., B. Feng, and Q. Sun, *Three-Dimensional Finite Element Modeling of Human Ear for Sound Transmission.* Annals of Biomedical Engineering, 2004. **32**(6): p. 847-859.
8. Gentil, F., et al., *The influence of muscles activation on the dynamical behaviour of the tympano-ossicular system of the middle ear.* Computer methods in biomechanics and biomedical engineering, 2013. **16**(4): p. 392-402.
9. Gentil, F., et al., *The Influence of the Mechanical Behaviour of the Middle Ear Ligaments: A Finite Element Analysis.* Proceedings of the Institution of Mechanical Engineers, Part H: Journal of Engineering in Medicine, 2011. **225**(1): p. 68-76.
10. Liu, Y., S. Li, and X. Sun, *Numerical analysis of ossicular chain lesion of human ear.* Acta Mechanica Sinica, 2009. **25**(2): p. 241-247.

11. Gentil, F., et al., *The biomechanical effects of stapes replacement by prostheses on the tympano-ossicular chain.* International journal for numerical methods in biomedical engineering, 2014. **30**(12): p. 1409-1420.
12. Ferris, P. and P.J. Prendergast, *Middle-ear dynamics before and after ossicular replacement.* Journal of Biomechanics, 2000. **33**(5): p. 581-590.
13. Sun, Q., et al., *Computer-integrated finite element modeling of human middle ear.* Biomechanics and Modeling in Mechanobiology, 2002. **1**(2): p. 109-122.
14. Gentil, F., et al., *Analysis of Eardrum Pathologies Using the Finite Element Method.* Journal of Mechanics in Medicine and Biology, 2014. **14**(3).
15. Berdich, K., et al., *Finite element analysis of the transfer of sound in the myringosclerotic ear.* Computer Methods in Biomechanics and Biomedical Engineering, 2016. **19**(3): p. 248-256.
16. Nielsen, A.H., et al., *The visible ear*, in *Faculty of Engineering and Science*. 2005, Aalborg University.
17. Hibbit, D.K., B.; Sorenson, P., *ABAQUS Analysis User's Manual Version 6.14-1*. 2014, Dassault Systèmes.
18. Gentil, F., *Estudo biomecânico do ouvido médio*. 2008, Universidade do Porto.
19. Mukherjee, S., A. Chawla, and B. Karthikeyan, *A review of the mechanical properties of human body soft tissues in the head, neck and spine.* Institute of Engineers Journal, 2006.
20. Henry, P.J.P.P.F., J. Rice, and A.W. Blayneyb, *Vibro-Acoustic Modelling of the Outer and Middle Ear Using the Finite-Element Method.* Audiology & Neurotology, 1999. **4**: p. 3-4.
21. Volandri, G., et al., *Biomechanics of the tympanic membrane.* Journal of biomechanics, 2011. **44**(7): p. 1219-1236.
22. Nishihara, S. and R. Goode, *Measurement of tympanic membrane vibration in 99 human ears*. in Huttenbrink KB, eds. Middle ear mechanics in research and otosurgery. Department of Oto-Rhino-Laryngology, Dresden University of Technology, Dresden, Germany, pp. 91–93, 1996.
23. Huber, A., et al., *The vibration pattern of the tympanic membrane after placement of a total ossicular replacement prosthesis*, in *Proceeding of the International Workshop on middle ear mechanics in research and otosurgery*. Dresden, Germany, pp. 219-22, 1997.
24. Lee, C.-F., et al., *Computer aided three-dimensional reconstruction and modeling of middle ear biomechanics by high-resolution computed tomography and finite element analysis.* Biomedical Engineering: Applications, Basis and Communications, 2006. **18**(05): p. 214-221.
25. Bentler, R.A., *External ear resonance characteristics in children.* Journal of Speech and Hearing Disorders, 1989. **54**(2): p. 264-268.
26. Shaw, E.A.G., *Transformation of sound pressure level from the free field to the eardrum in the horizontal plane.* Journal of The Acoustical Society of America, 1974. **56**(6).
27. Voss, S.E., et al., *Acoustic responses of the human middle ear.* Hearing Research, 2000. **150**(1–2): p. 43-69.
28. Aibara, R., et al., *Human middle-ear sound transfer function and cochlear input impedance.* Hearing Research, 2001. **152**(1–2): p. 100-109.
29. Wiener, F.M. and D.A. Ross, *The pressure distribution in the auditory canal in a progressive sound field.* The Journal of the Acoustical Society of America, 1946. **18**(2): p. 401-408.
30. Mehrgardt, S. and V. Mellert, *Transformation characteristics of the external human ear.* The Journal of the Acoustical Society of America, 1977. **61**(6): p. 1567-1576.
31. Gardner, M.B. and M.S. Hawley, *Network representation of the external ear.* J Acoust Soc Am, 1972. **52**(6): p. 1620-8.
32. VanPutte, C.L. and R.R. Seeley, *Seeley's anatomy & physiology*. 10th ed. 2014, New York, NY: McGraw-Hill.

33. Kelly, D.J., P.J. Prendergast, and A.W. Blayney, *The effect of prosthesis design on vibration of the reconstructed ossicular chain: A comparative finite element analysis of four prostheses.* Otology & Neurotology, 2003. **24**(1): p. 11-19.
34. Stenfelt, S., *Acoustic and physiologic aspects of bone conduction hearing.* 2011.
35. Homma, K., et al., *Effects of ear-canal pressurization on middle-ear bone- and air-conduction responses.* Hearing Research, 2010. **263**(1–2): p. 204-215.
36. Berkow, R., et al., *The Merck manual home edition*. 2000, Merck & Co.,: Whitehouse Station, NJ.
37. Ney, D.F., *Cerumen impaction, ear hygiene practices, and hearing acuity: Nurses should play a more active role in identifying cerumen impactions and other causes of hearing loss.* Geriatric Nursing, 1993. **14**(2): p. 70-73.

Figure 1

Click here to download Figure Fig 1.pdf

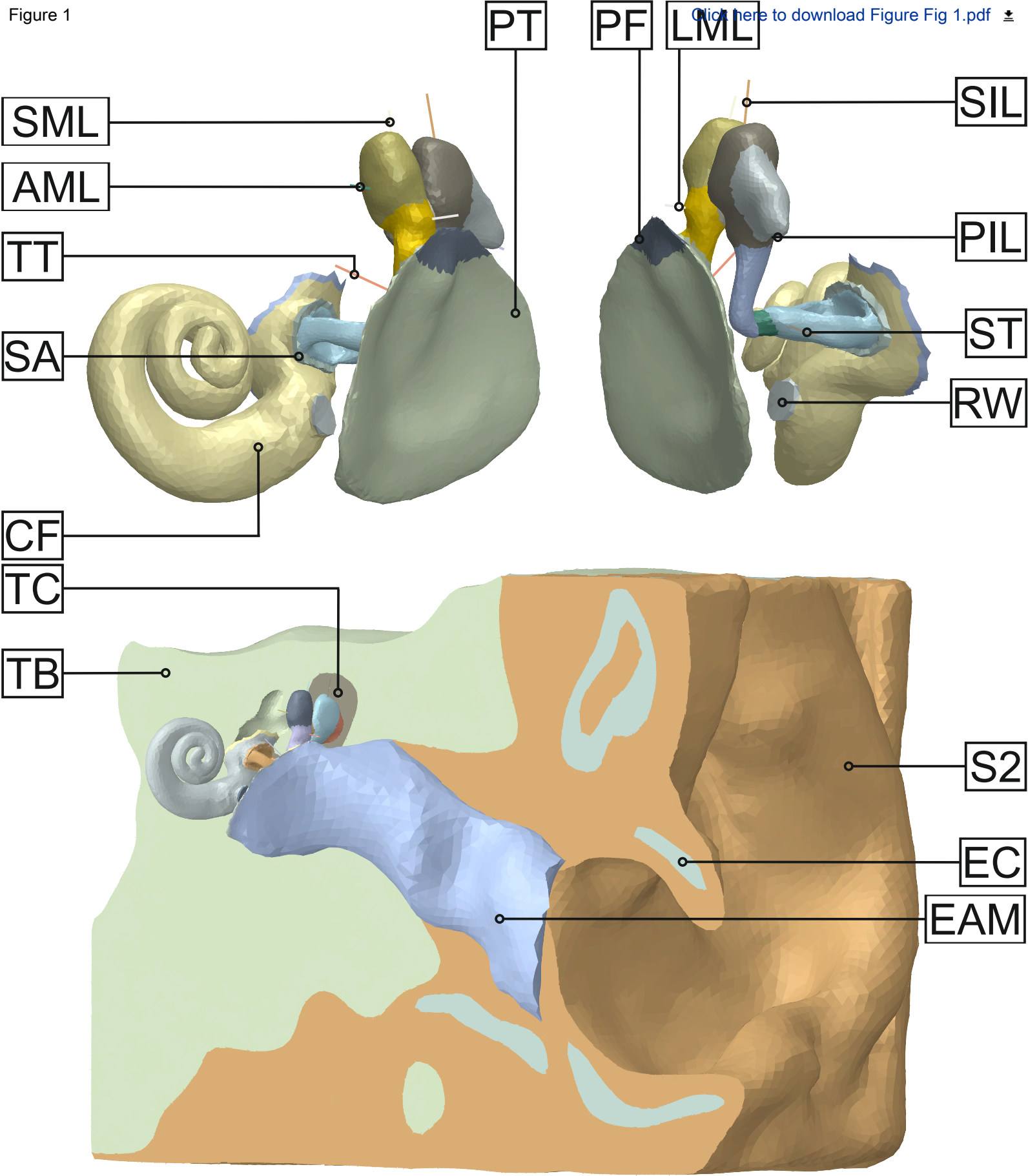

Figure 2

Click here to download Figure Fig 2.pdf

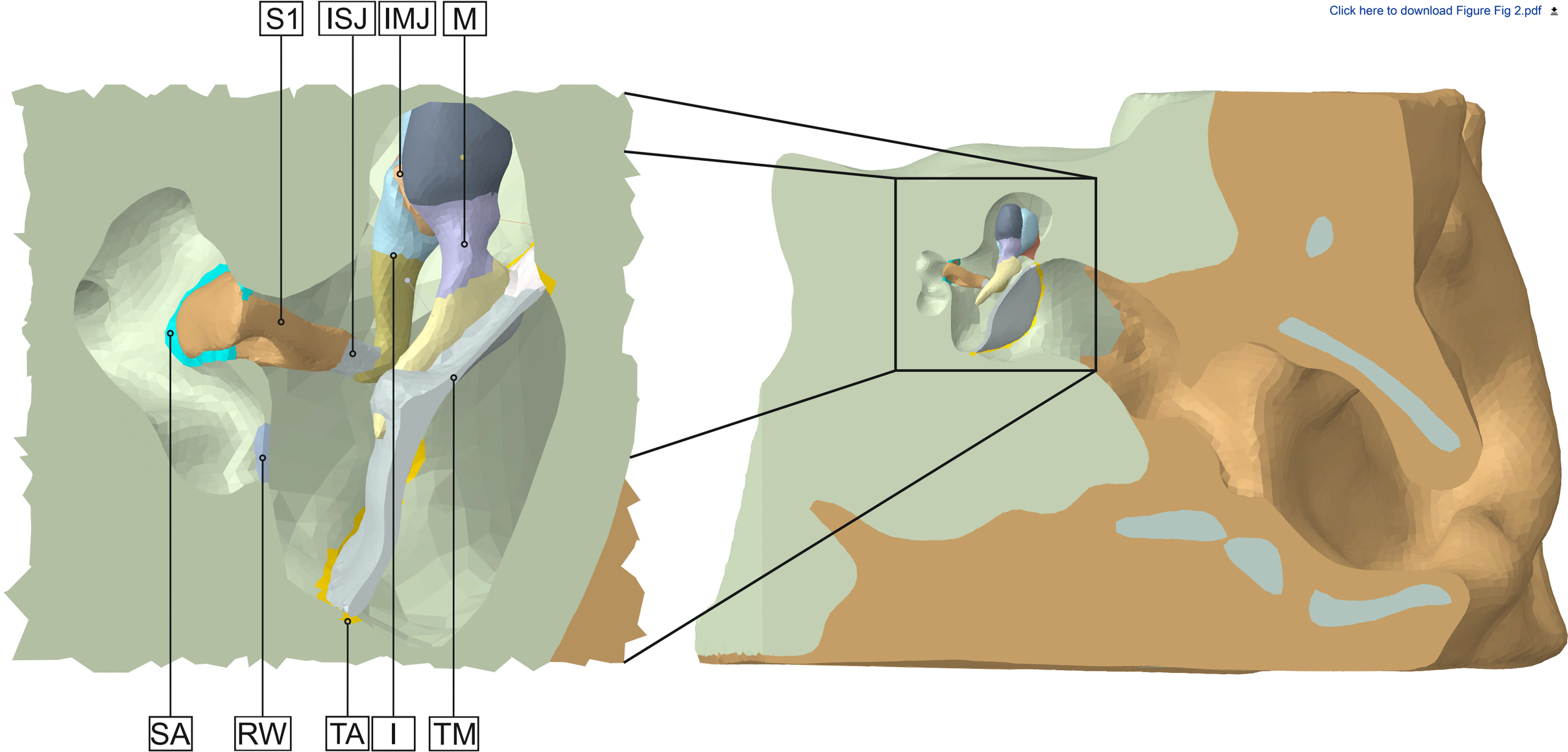

Figure 3

Click here to download Figure Fig 3.pdf

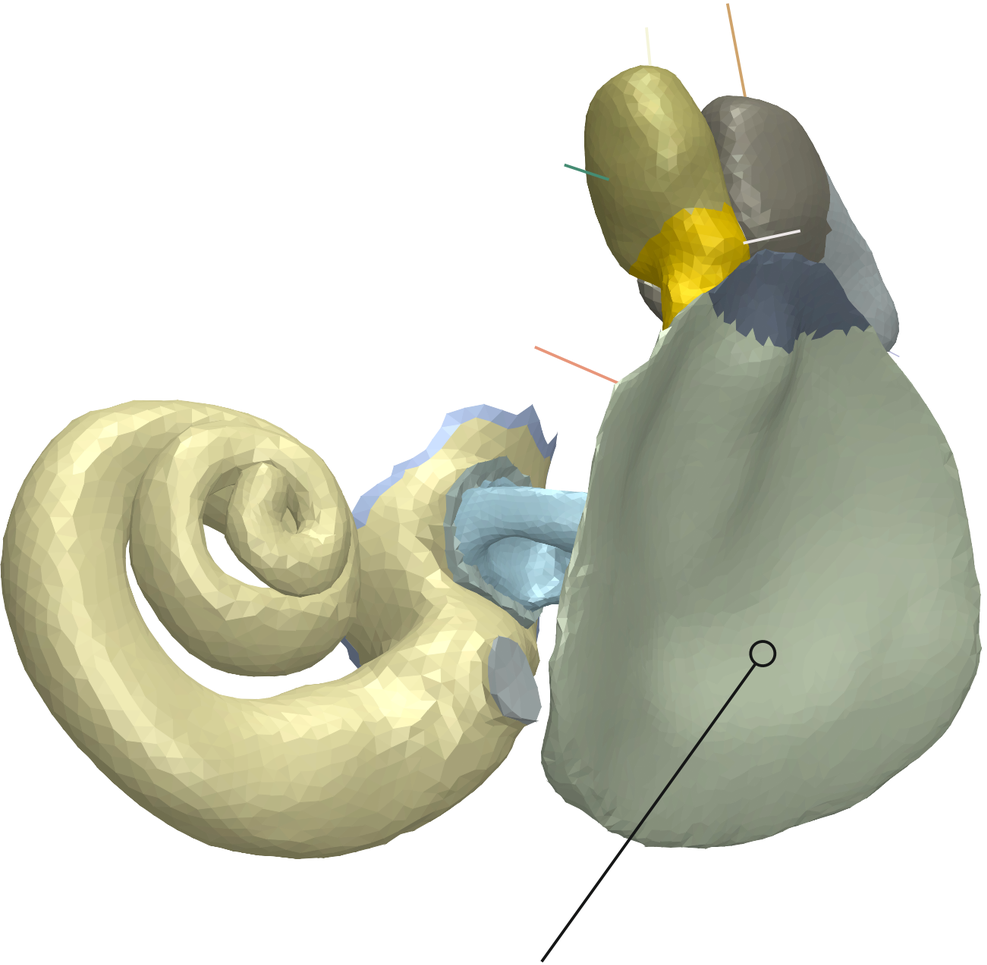

Acoustic pressure in simple model

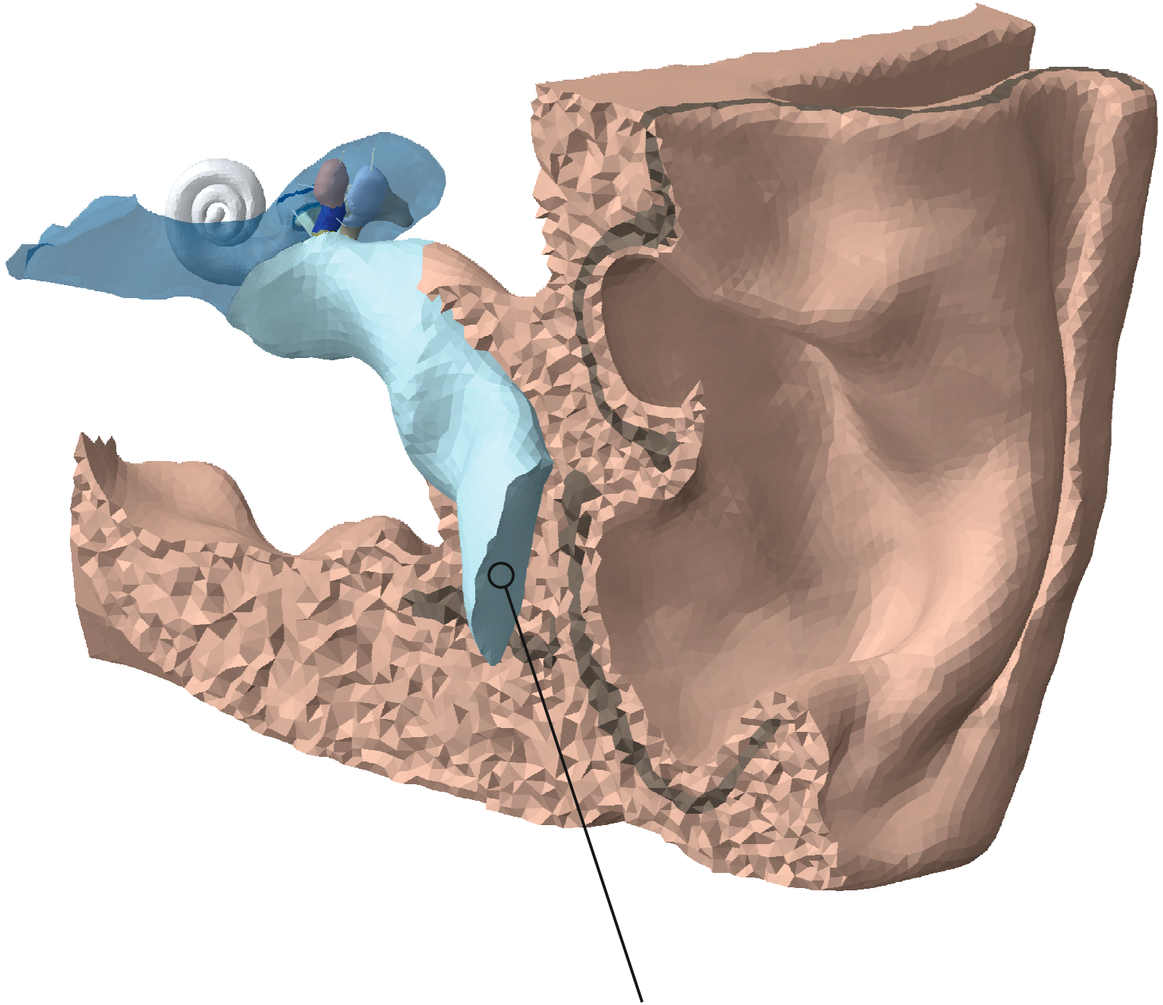

Acoustic pressure in full model

Figure 4

Click here to download Figure Fig 4.pdre

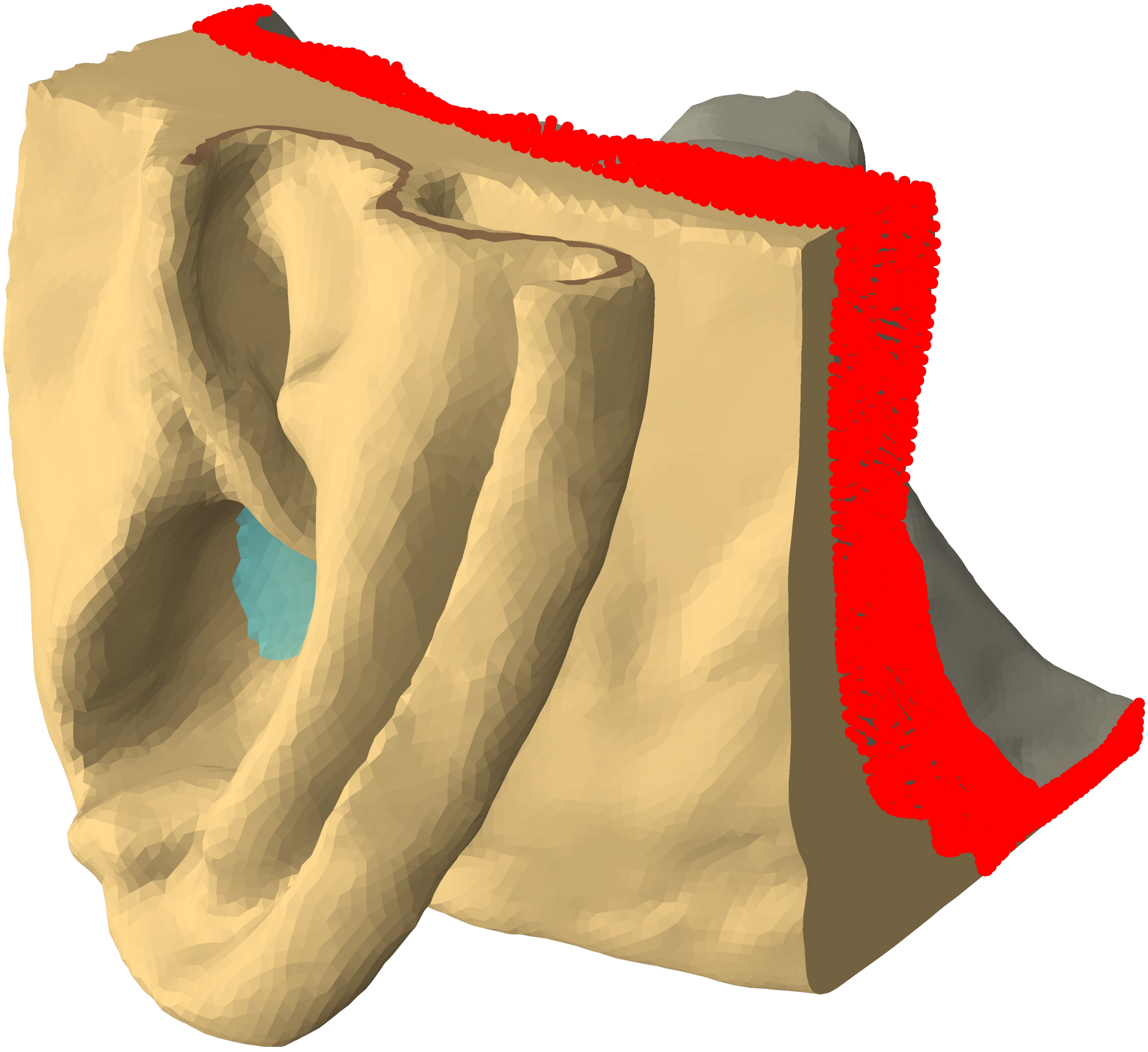

Figure 5

Click here to download Figure Fig 5.pdf

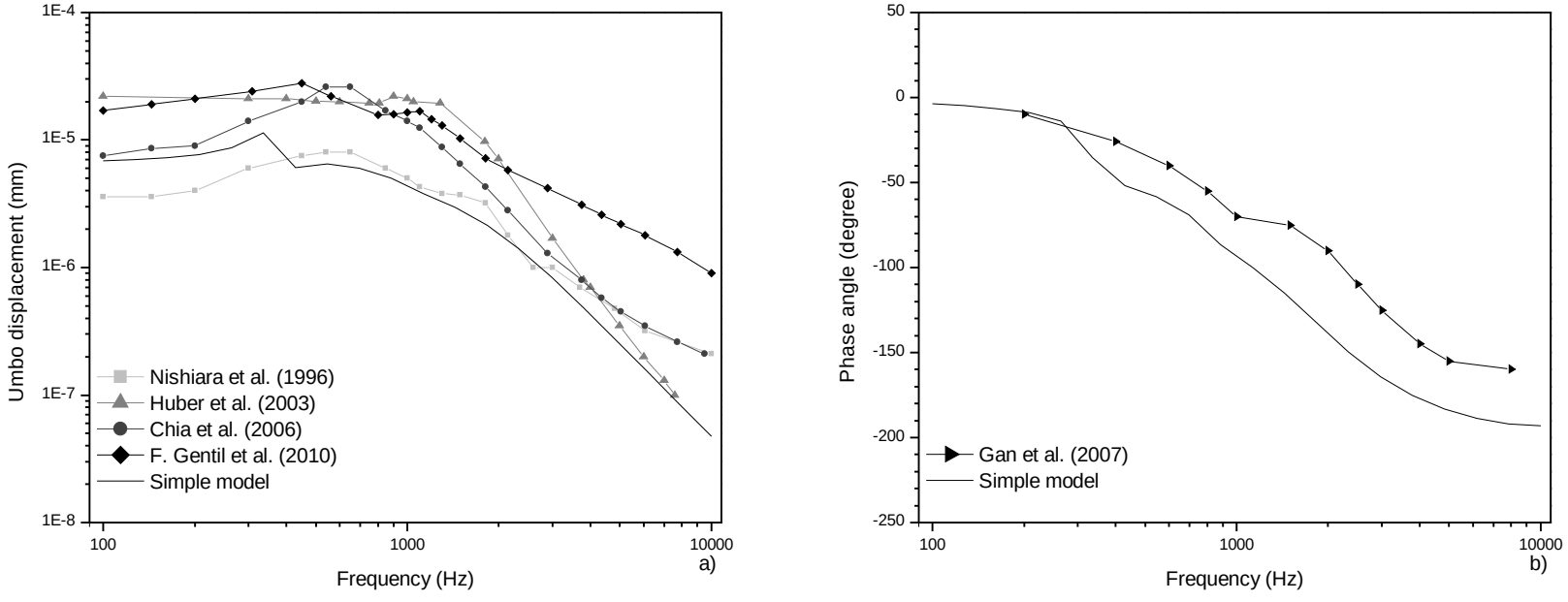

Figure 6

Click here to download Figure Fig 6.pdf

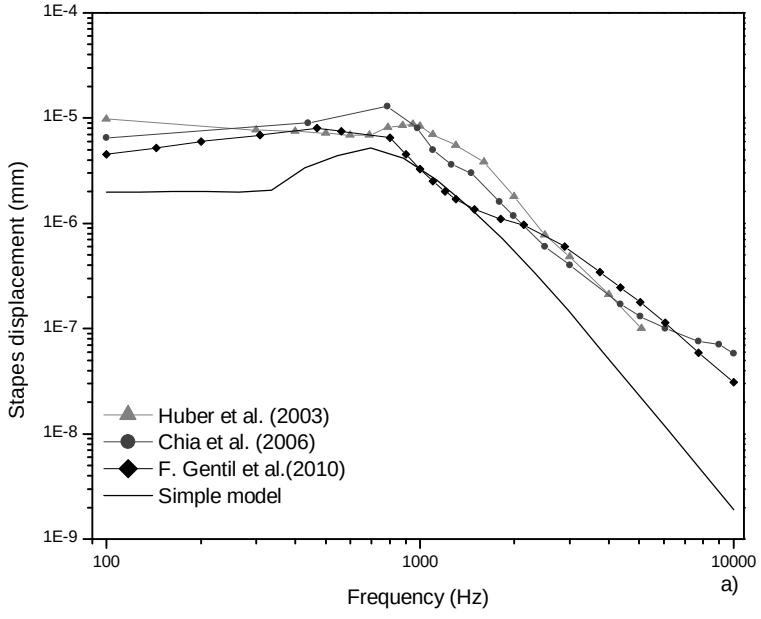

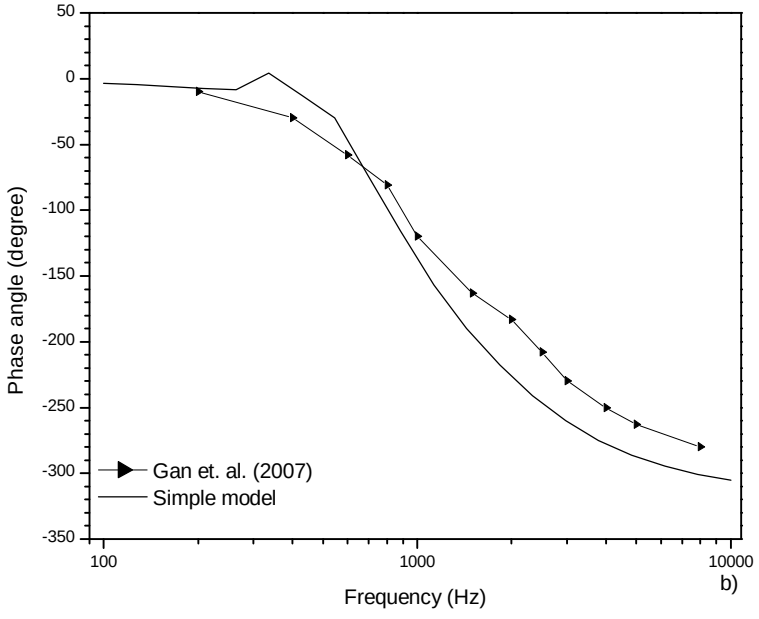

Figure 7

Click here to download Figure Fig 7.pdf

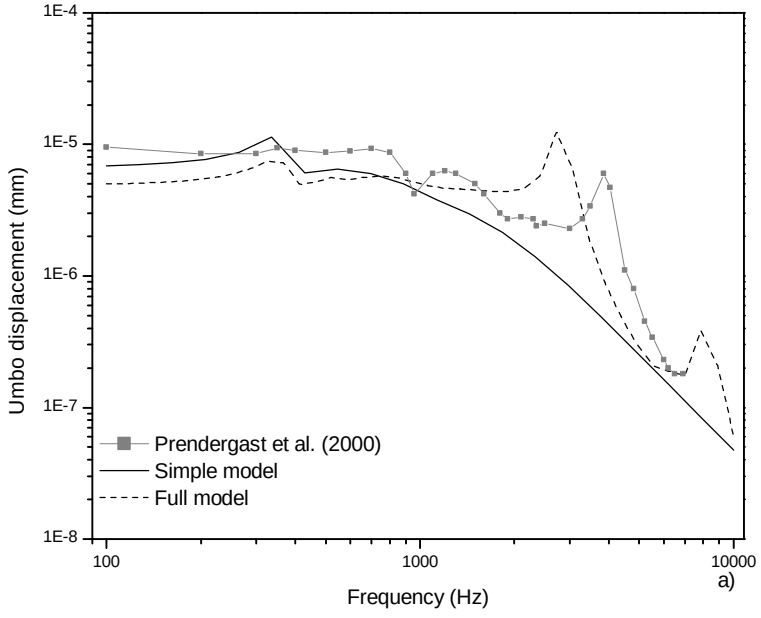

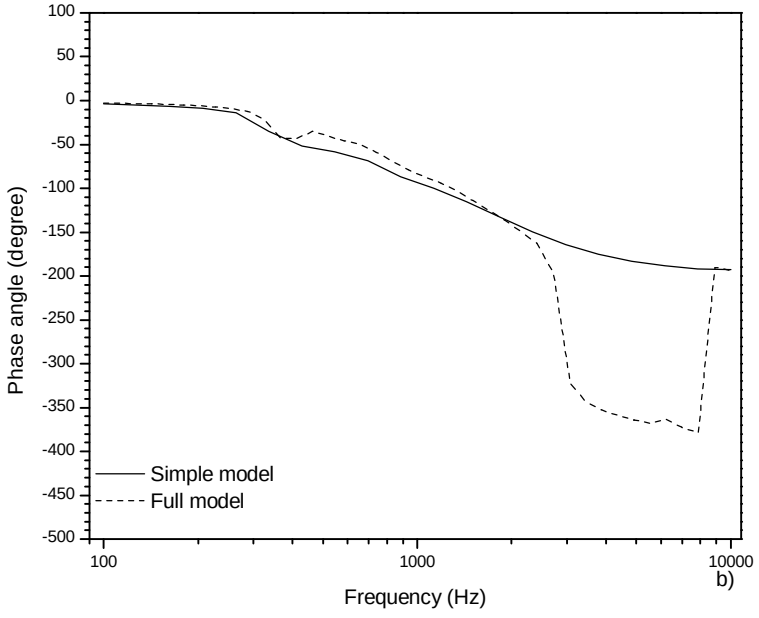

Figure 8

Click here to download Figure Fig 8.pdf

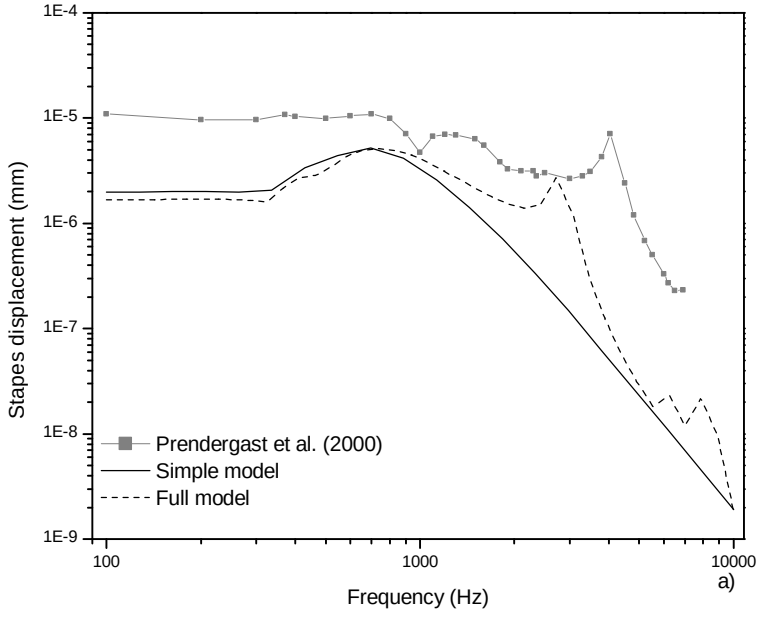

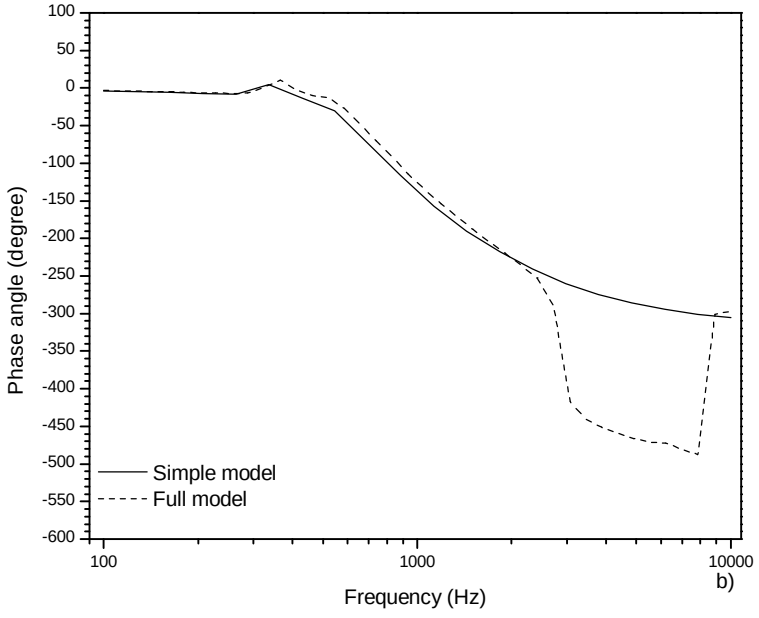

Figure 9

Click here to download Figure Fig 9.pdf

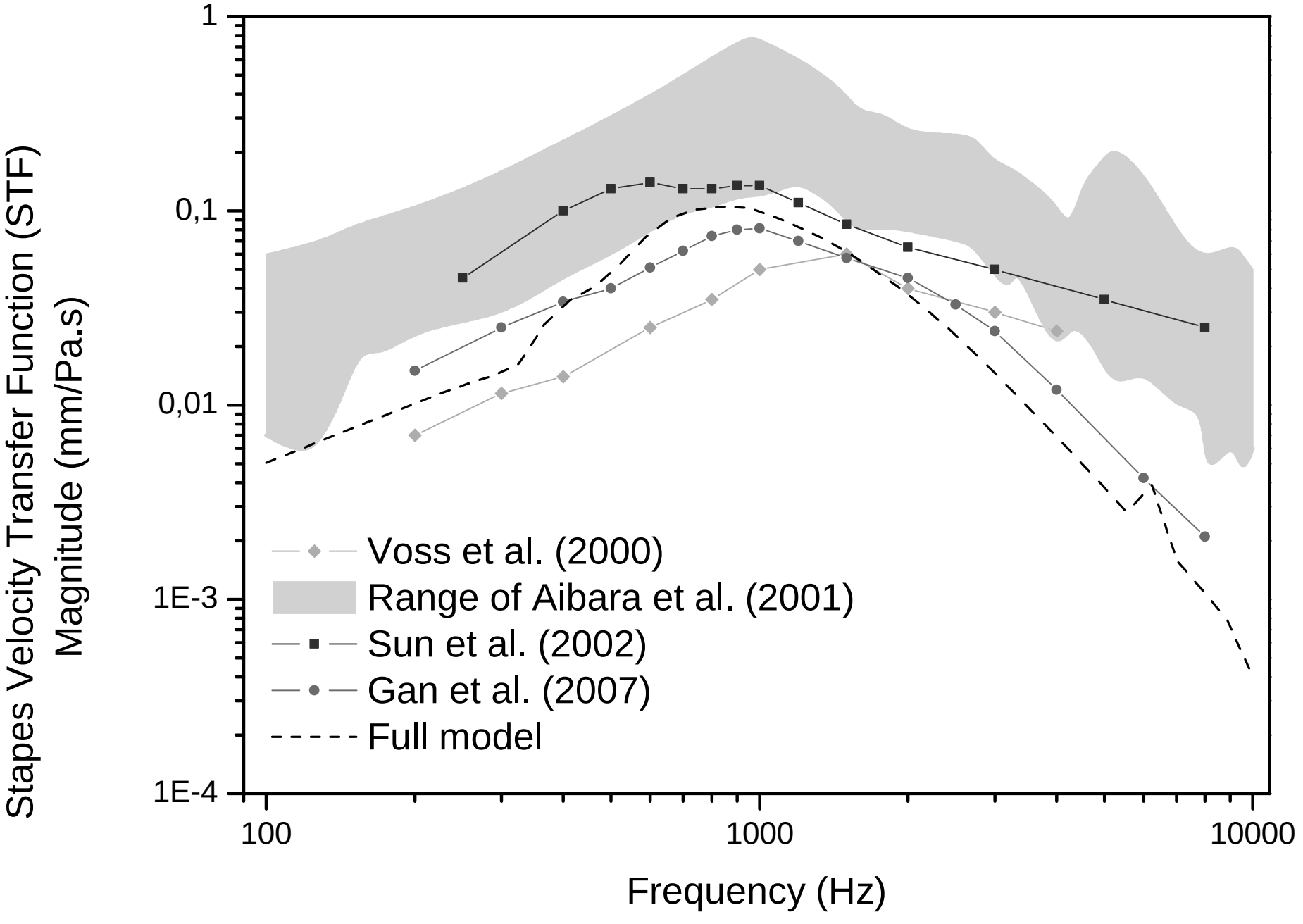

Figure 10a

Click here to download Figure Fig 10a.pdf

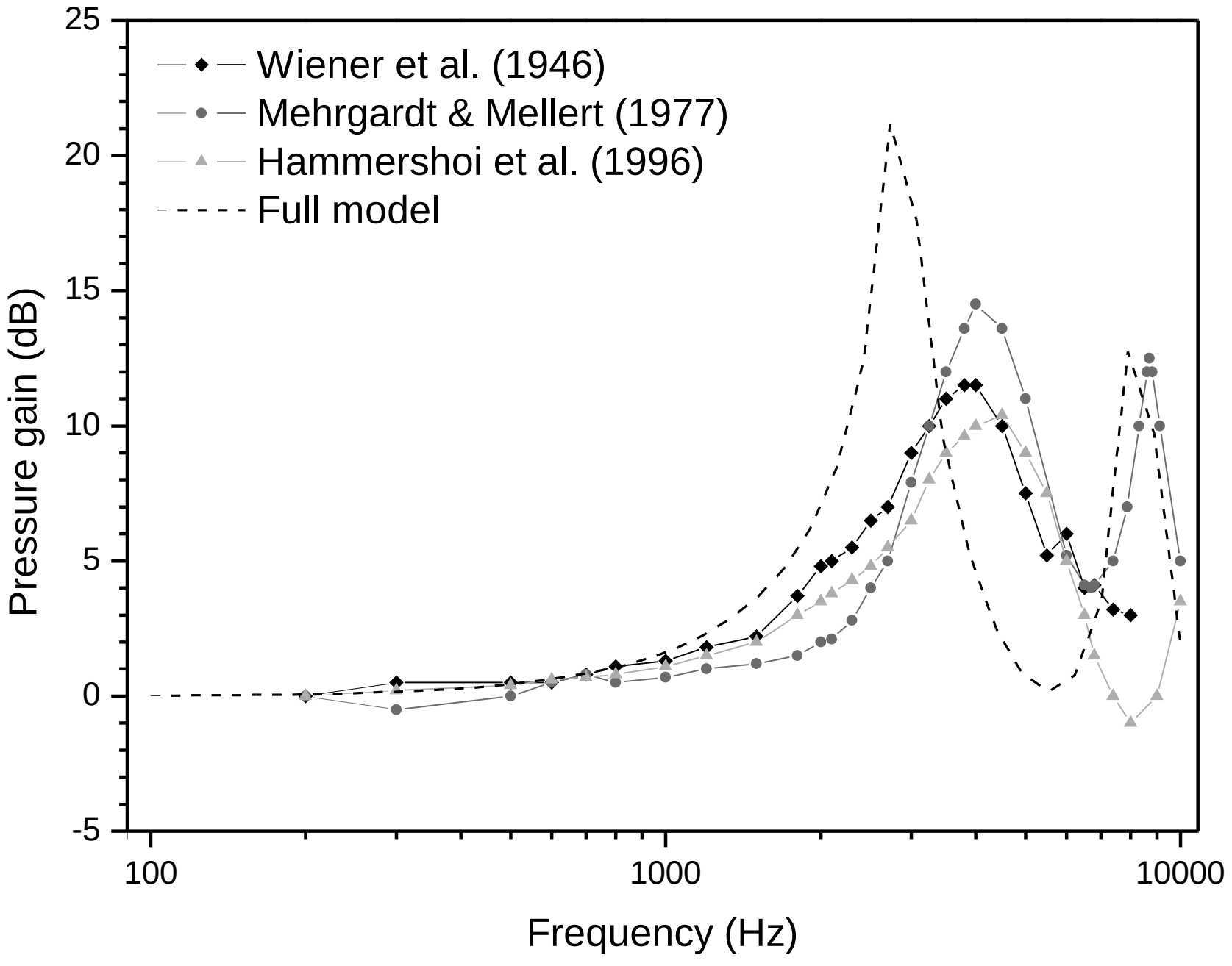

Figure 10b